Article

Not peer-reviewed version

# High salinity tolerance of Zn-rich CNx in the photocatalytic treatment of wastewater

Hongyu Chen , Lei Wang , Suiyi Zhu * , Jiancong Liu

Posted Date: 27 May 2024

doi: 10.20944/preprints202405.1750.v1

Keywords: Photocatalyst, Carbon nitride, Salinity tolerance, Wastewater treatment, Degradation

*Article*

# High Salinity Tolerance of Zn-Rich $CN_x$ in the Photocatalytic Treatment of Wastewater

**Chen Hongyu [1], Wang Lei [2,3], Zhu Suiyi [4,*] and Liu Jiancong [2]**

[1] School of Environment, Northeast Normal University, Changchun, 130117, P. R. China;
[2] School of Materials and Environmental Engineering, Institute of Urban Ecology and Environment Technology, Shenzhen Polytechnic University, Shenzhen 518055, P. R. China;
[3] Eco-Environmental Science Center (Guangdong, Hong-Kong, Macau), Guangzhou 510555, P. R. China;
[4] College of Resources and Environment, Zhongkai University of Agriculture and Engineering, Guangzhou, Guangdong, P. R. China.
* Correspondence: papermanuscript@126.com

**Abstract:** physicochemical methods was effective for the degradation of organics, but was highly hampered by the salt coexist in the complex wastewater matrix, resulting in low degradation dynamics. In this study, ZnO loaded carbon nitride (Zn-$CN_x$) was synthesized and exhibited an excellent performance for 2,4-dichlorophenol (2,4-DCP) degradation (0.63 mg/L/min) in photcatalysis system. The doping of Zn into $CN_x$ contributed to the increased light absorption of the catalyst and the optimized electron transport pathways. The quenching experiment results proved that the superoxide radicals ($\cdot O_2^-$) played a dominant role and hydroxyl radical (·OH) played a secondary role. Notably, the 2,4-DCP removal increased slightly with increasing salt content. As the initial pH increased from 3 to 11, the first-order degradation kinetic constants increased significantly, and the final pH was equilibrized in the range of 6.01-6.59. This study provided a high performance catalyst for photcatalysis and the mechanism for the effective degradation of 2,4-DCP under high salinity condition.

**Keywords:** photocatalyst; carbon nitride; salinity tolerance; wastewater treatment; degradation

## Highlights

1. Zn-rich CNx photocatalyst had desirable salinity tolerance;
2. Heterojunction photocatalyst occurred on CNx by doping Zn;
3. Zn doping showed superior to that of Co, Ag, Mo, and Bi;
4. Degradation pathway of 2,4-DCP were analyzed.

## 1. Introduction

With the gradually expandssion of the paper, printing and dyeing, pharmaceutical and pickled food industries, a large and complex amount of high salt organic wastewater was produced [1,2]. As reported, the wastewater produced during the production of herbicide 2,4-dichlorophenoxyacetic acid (2,4-D) contained 2,4-dichlorophenol (2,4-DCP) up to 800-1200 mg/L, while the NaCl concentration reached 55.0-65.0 g/L [3]. In view of the highly toxicity, ecologically persistence, accumulation and mobilit, it was harmful to the ecosystem and public health, which needed to be strictly controlled and properly handled in China, the United States and other European countries [3]. However, its high salt content characteristics had a significant negative impact on aerobic and anaerobic bacteria to limi the application of biological treatment processes [4].

At present, a number of physicochemical methods were considered to have an advantage for the treatment of this type of wastewater, such as fenton, membrane, evaporative crystallization, electrocatalysis and photocatalysis, etc. It has been demonstrated that the decomposition of $H_2O_2$ catalyzed by $Fe^{2+}$ produced ·OH ($E^0$=2.70 $V_{NHE}$) with strong oxidizing ability to indiscriminately attack organic matter, and the dissolved oxygen gained electrons under catalytic conditions to produce $\cdot O_2^-$

 doi:10.20944/preprints202405.1750.v1



($E^0$=1.06 $V_{NHE}$) to selectively attack electron-rich groups [5,6]. Physical processing enabled efficient phase transfer of organic matter. Efficient removal of organic matter without being affected by salinity was the goal pursued. However, the material had a high surface energy, which tended to induce salt precipitation and salt crystallization in the indication. This phenomenon was observed in applications such as membrane filtration and electrocatalysis [7,8]. The Fenton method and evaporation crystallization required a large amount of reagents and additional energy. Compared with the above, photocatalytic technology could continuously and efficiently decompose organic matter in water under the condition of lower energy consumption, which demonstrates certain advantages in salt-containing wastewater treatment.

However, there were some disadvantages of photocatalytic process for treating high salt wastewater. Specifically, the active sites on the catalyst surface was used to enhance the capture and oxidative degradation of organic matter in water on the one hand, and the capture of active species in water to enhance the generation of free radicals on the other hand [9]. Under high salt stress, salt occupied the surface active sites and prevented subsequent adsorption-catalyzed degradation of organic matter. This was a typical catalyst deactivation phenomenon [10]. Reducing the adsorptive active sites while enhancing the generation of free radicals was the focus of current catalyst research and development.

As previously reported, we loaded metals onto carbon nitride by thermal condensation method to prepare stable composite catalysts with high catalytic activity for 2,4-DCP removal from highly chlorine environment. In this study, effects of other parameters such as catalyst, salinity, pH value, 2,4-DCP concentration on the degradation process were evaluated and the degradation pathway of 2,4-DCP was deduced. Further, the reactive oxygen species evolution and the 2,4-DCP degradation pathways were proposed based on quenching experiment and product analysis. In conclusion, this study revealed the possible mechanism of high-salt wastewater treatment using photocatalysis.

## 2. Materials and Method

### *2.1. CNs Synthesis*

The CNs were synthesized as follows. First, mixed 6.82 g $ZnCl_2$ and 25.20 g melamine at the mol ratio of 4:1 in 300 mL 0.35 wt.% HCl solution at 90-95 °C and then agitated for 30 min. Second, freeze-dried the mixture for 2 days, and then calcinated at 400-500 °C for 4h, to produce powdered material. Third, washed the materials by water and ethanol several times, and then dried overnight. A pink powder was generated and named as Zn-$CN_x$. In the control experiment, the added Zn salt was replaced by Co, Ag, Mo, and Bi salts, respectively, according to the above steps. The corresponding products were named as Co-$CN_x$, Mo-$CN_x$, Ag-$CN_x$ and Bi-$CN_x$.


**Figure 1.** Flow chart for preparing metallic CNs particles.

### *2.2. Photocatalytic Experiment*

The prepared $CN_x$ was used for removing 2,4-DCP from salt wastewater. First, mixed 20 mg CNx into 200 mL wastewater containing 100 mg/L 2,4-DCP. Second, agitated the wastewater at 500 rpm for 30 min. Third, opened the mercury lamp to start the photocatalytic experiment, and then took 1 mL wastewater samples at a given interval, following by quenching with methanol. The rest 2,4-DCP concentration was determined by HPLC. Control experiments were performed by varying

 doi:10.20944/preprints202405.1750.v1



the salt dosage, the initial pH and the 2,4-DCP concentrations in the range of 0.58‰-11.70‰, pH 3.0-11.0 and 20-200 mg/L, respectively. The experiment was repeated three times, and the average data was reported.

### *2.3. Characterization*

The prepared $CN_x$ were characterized by SEM, XRD, FTIR, UV-vis, PL and XPS, separately. The generated intermediates in the degradation experiment were analyzed by using UPLC.

## 3. Results and Discussion

### *3.1. Metallic CNs Characterization*

Six $CN_x$ were prepared in the experiment and showed typical peaks of $CN_x$ at $2\theta = 10^o$ and $80^o$ (Figure 2a). However, sharp peaks of CoO, elemental Ag, $MoO_3$, elemental Bi and ZnO were found on the corresponding $CN_x$. This revealed the formation of metallic $CN_x$. After the treatment for 120 min, nearly 75.60% 2,4-DCP were removed in the presence of Zn-rich $CN_x$, higher than these with the addition of pure $CN_x$, and Co, Ag, Mo, and Bi doped $CN_x$ (Figure 2b). Such degradation date fitted good with the pseudo-first kinetic model with the regression coefficients of > 0.99. However, the corresponding degradation rates by adding Co, Ag, Mo, and Bi-doped $CN_x$ were in the range of 0.0044-0.0051 $min^{-1}$, nearly half of that with the addition of Zn-rich $CN_x$. This demonstrated that the doping of Zn apparently enhanced the photocatalytic performance of $CN_x$.

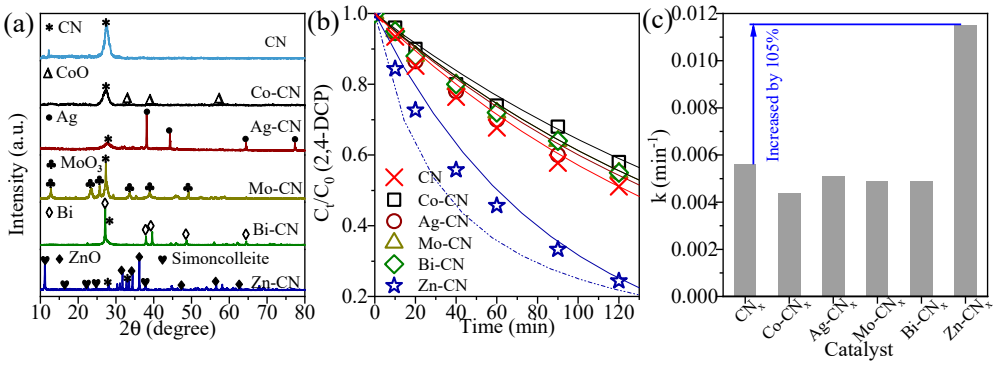


**Figure 2.** (a) XRD pattern of metallic CNs, (b) photocatalytic degradation of 2,4-DCP by metallic CNs and (c) the related kinetic constant.

### *3.2. Photocatalytic Conditions Optimization*

The Zn-rich $CN_x$ showed superior performance in the degradation of 2,4-DCP in salt wastewater. Figure 3a showed that the degradation efficiency of 2,4-DCP slightly varied in the salt dosage of 0.58‰-11.7‰, demonstrating that Zn-rich $CN_x$ showed good stability in the high-salt wastewater. However, with the decrease of pH from 9 to 3, the degradation efficiency also dropped from 84.66 to 70.08%. But when the initial pH was increased from 9 to 11, the degradation efficiency was considerably increased to 99.41% (Figure 3b). After reaction, the final pH was also equilibrized in the range of 6.01-6.59 (Figure 3c). Without the addition of Zn-rich $CN_x$, the equilibrium pH was steadily dropped. The related mechanism will be discussed in section 3.4.

As the increase of the initial 2,4-DCP concentration in the range of 20.00-200.00 mg/L, the corresponding degradation efficiency was also dropped from 100.00 to 51.90% (Figure 3d). The high removal of 103.81 mg/L 2,4-DCP occurred with the addition of 200 mg/L 2,4-DCP (Figure 3e). Without the photocatalyst, the direct adsorption of 2,4-DCP onto the Zn-rich $CN_x$ were 2.09, 9.00, 12.19 and 13.00 with the addition of 20.00, 50.00, 100.00 and 200.00 mg/L 2,4-DCP (Figure 3f), in accordance with the removal of 2.09%, 1.80%, 1.19% and 0.68% 2,4-DCP from the wastewater. This demonstrated that the photocatalytic degradation played a key role in the removal of 2,4-DCP from salt wastewater.

 doi:10.20944/preprints202405.1750.v1



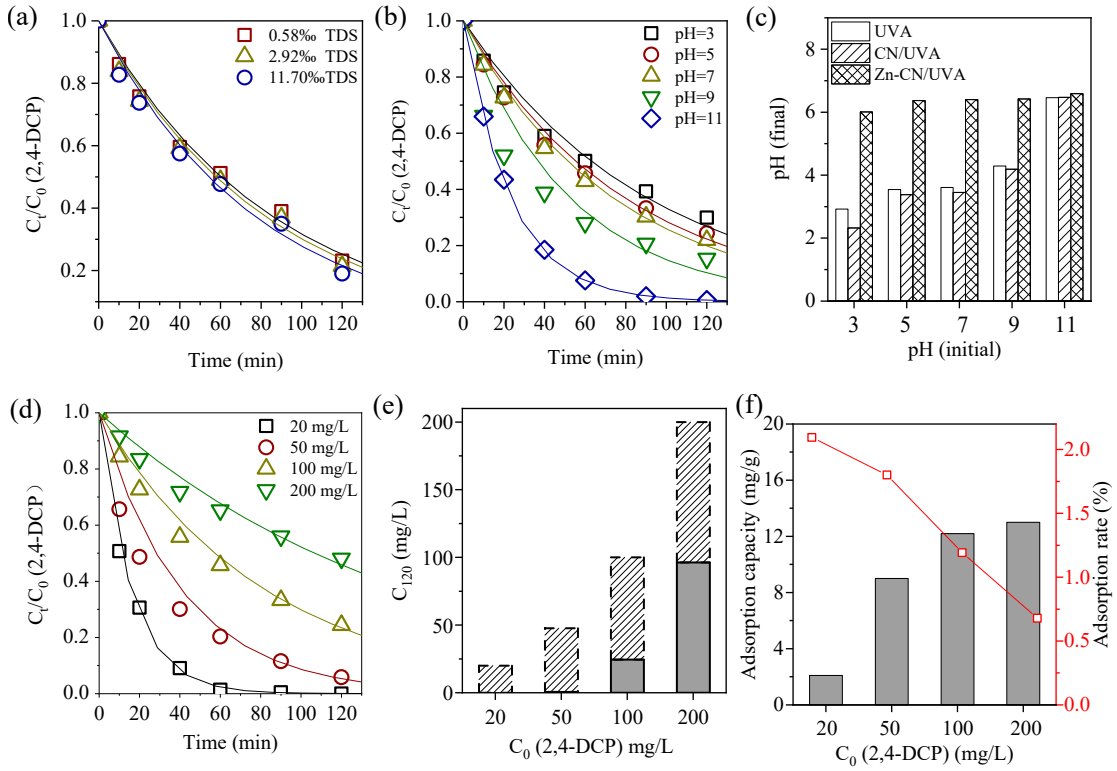


**Figure 3.** Degradation of 2,4-DCP. (a) salt concentration, (b) initial pH, (c) final pH value, (d) initial concentration, (e) final concentration, (f) direct adsorption.

### *3.3. Zn-Rich CNs Materials Characterization*

The Zn-rich $CN_x$ was aggregated particles (Figure 4a), and kept sharp peaks of $CN_x$ at the wavenumbers of 1451, 1400 and 1316 $cm^{-1}$ (Figure 4b). However, the peaks at 1100, and 733 $cm^{-1}$ shifted to low-value and few peaks at 3080, 1240 and 805 $cm^{-1}$ disappeared, belong to the conjunction of ZnO onto $CN_x$ via −NH and −OH bonds. The XPS spectra showed two peaks of Zn 2p at 1022.0 and 1045.1 eV (Figure 3c). For C 1s, the peak at 288.4 and 284.8 eV became intensified (Figure 3d), demonstrating that more −COOH and C−C sites were exposed with the addition of Zn. According, the N1s peaks of C−N=C bond at 398.7 eV also raised (Figure 3e), and the peak of $N-(C)_3$ bond at 400.4 eV disappeared. However, for O1s, a new peak at 533.4 eV belonged to adsorbed $O_2$ and/or water. Such results demonstrated the doping of Zn into $CN_x$ and the corresponding variation of functional sites.

 doi:10.20944/preprints202405.1750.v1



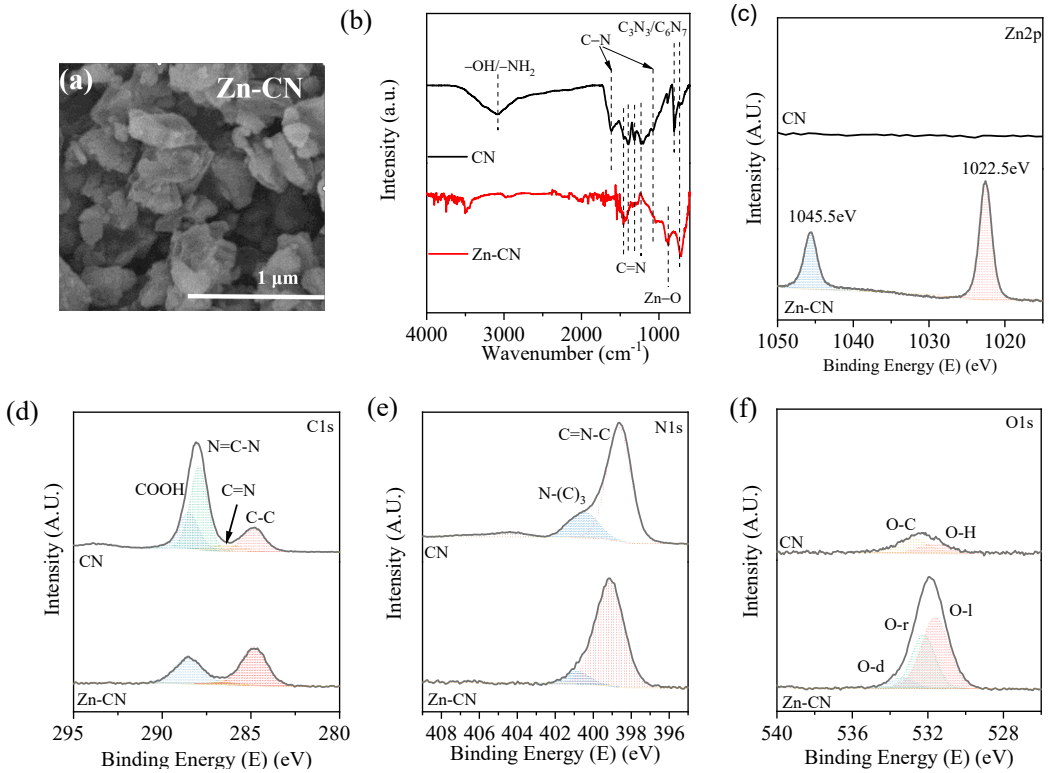


**Figure 4.** (a) SEM images, (b) XRD patterns, (c) FTIR, high resolution (d) Zn 2p, (e) C 1s, (f) N 1s, and (g) O 1s XPS spectra.

### *3.4. Photocatalytic Mechanism Analysis*

In the photocatalysis system, the photon was adsorbed by $CN_x$, and then converted into a pair of electron-hole. The generated hole only oxidized the adsorbed organics on $CN_x$ surface. But the electron was transited to $CN_x$ surface and then captured by $OH^-$ and oxygen groups, with the formation/releasing of free radicals into the wastewater. This started the oxidation of organics in wastewater. Given that the direct adsorption of 2,4-DCP on $CN_x$ was low (Figure 3f), the generated free radicals played positive roles in the degradation of 2,4-DCP in the salt wastewater.

The doping of Zn into $CN_x$ showed two advantages. First, the photo absorbance of $CN_x$ increased and strengthened. The doped ZnO restructured the surface sites of $CN_x$, and then more ZnO and oxygen vacancy sites were exposed to surface. Accordingly, the band-gap energy raised from 2.74 eV to 3.35 eV (Figure 5a), and the UV-vis absorbance in the range of 300-360nm also became intensified (Figure 5b), demonstrating that more photons were adsorbed by Zn-rich $CN_x$. Second, a heterojunction structure was formed in Zn-rich $CN_x$ and steadily increased the production of free radicals. For example, an electron was generated on the conduction band of ZnO, but moved to the valence band of $CN_x$ in the heterojunction structure, not to that of ZnO (Figure 5c). This extended the transportation distance of photo-induced electron/hole pairs. Thereby, more photo-induced electron transported to the surface and then involved in the production of free radicals. No heterojunction structure was formed in the doping of Co, Ag, Mo and Bi into $CN_x$, and thereby the corresponding removal efficiencies of 2,4-DCP were low.

Preprints.org (www.preprints.org) | NOT PEER-REVIEWED | Posted: 27 May 2024 doi:10.20944/preprints202405.1750.v1



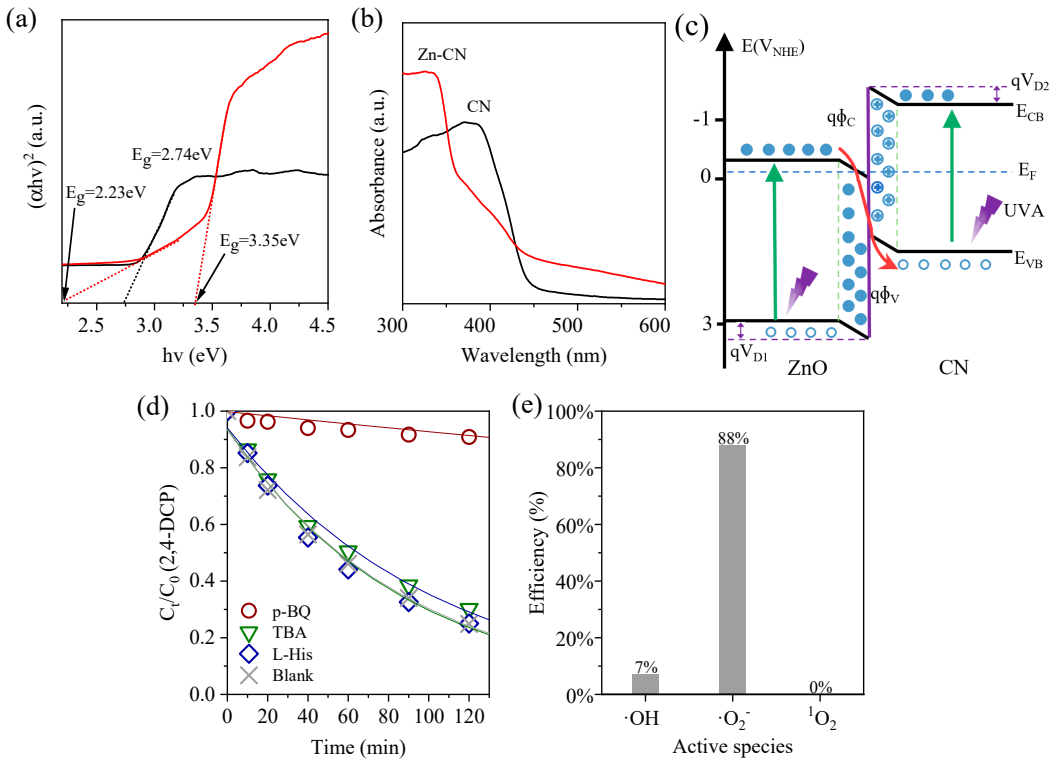


**Figure 5.** (a) Kubelka-Munk spectra, (b) UV-vis spectra, (c) PL spectra, (d) charge transfer process of Zn-rich CNs, (e) scavenger effect, and (f) the corresponding free radicals.

2,4-DCP was targeted to determine the photocatalytic performance of $CN_x$. It has a benzene ring with two chlorine and one hydrogen group, and was also adsorbed onto the Zn-rich $CN_x$. Such adsorption performance was mainly affected by the experimental conditions, e.g., the salt condition, the initial pH, and the initial concentration. For instance, at high salt condition, the free anions and cations were also adsorbed onto the $CN_x$ surface, in comparison with 2,4-DCP. This led to the decrease of the adsorption capacity of 2,4-DCP. Similarly, the initial pH also varied the structure and the $pH_{zpc}$ of 2,4-DCP. However, the removal efficiency of 2,4-DCP onto the Zn-rich $CN_x$ via adsorption, was relatively low, comparing with that of photocatalytic degradation. This demonstrated that the oxidation of free radicals predominated the removal of 2,4-DCP.

The quench experiment showed that only two free radicals of $\cdot O_2^-$ and ·OH were generated (Figure 5d). Especially, the radical $\cdot O_2^-$ occupied by 88% of 2,4-DCP removal, whilst the radical ·OH only contributed the removal of 7% 2,4-DCP (Figure 5e). The radical ·OH can be converted to the radical Cl·, to continue the oxidation of 2,4-DCP. Thereby, the photocatalytic degradation of 2,4-DCP by the Zn-rich $CN_x$ was stable in high salt wastewater. With the raise of wastewater pH, more $OH^-$ were involved in the production of free radicals, and then steadily decreased the equilibrium pH.

The degradation of 2,4-DCP mainly included two ways. One of which is the direct decomposition by UVA, which did second role in the 2,4-DCP removal. The adjacent position of hydroxyl group on 2,4-DCP, was firstly activated by UVA, to form two intermediates, 3,5-Dichloro-2-(2,4-dichlorophenoxy)phenol and 2,4-Dichlorophenoxycarboxylic acid. The intermediates were unstable and then converted to P-chlorophenol and o-chlorophenol , and p-phenol and o-phenol, respectively. Under such condition, the benzene ring did not open, instead, was combined in the form of 3,5-Dichloro-2-(2,4-dichlorophenoxy)phenol. The following decomposition commonly experienced several hours. The other is the photocatalytic degradation by UVA in the presence of Zn-rich $CN_x$, predominating the 2,4-DCP removal. With the treatment, the adequate of free radicals, e.g., $\cdot O_2^-$ and ·OH, were generated and attacked randomly the chlorine and hydroxyl groups. This simultaneously started the dechloridation and the ring opening of benzene ring, with the generation of abundant byproducts, e.g., maleic/fumaric acids, trihydroxyethylene, propanoic acid, acetic acid

 doi:10.20944/preprints202405.1750.v1



and oxalic acid. As the generation of free radicals continued, the rapid decomposition of 2,4-DCP and its byproducts also proceeded, to release free chloridion and carbonate into wastewater.

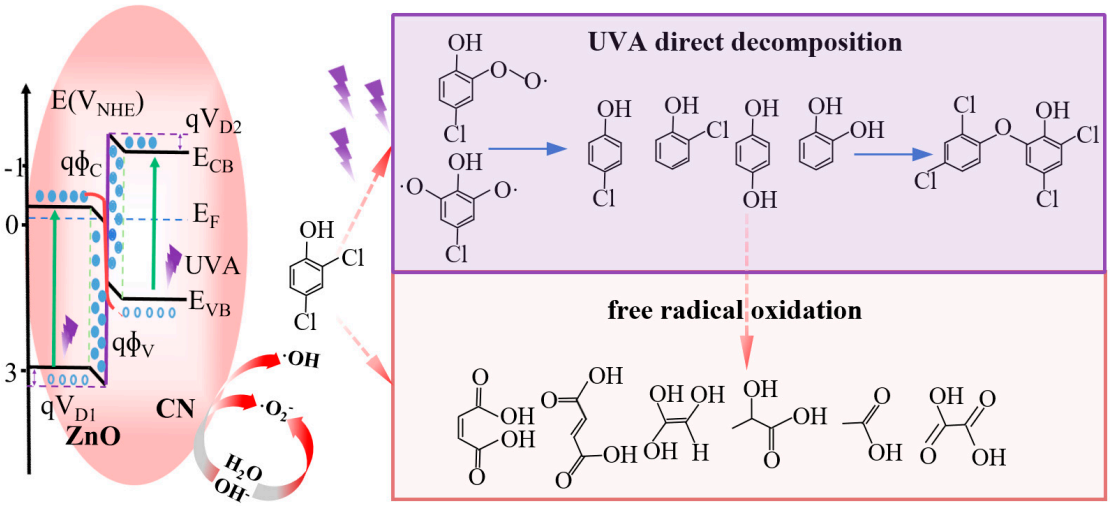


**Figure 6.** Derivation of 2,4-DCP degradation pathways in photolysis (UVA) and photocatalysis (Zn-CN/UVA) systems.

*3.5. Prospectives*

The Zn-rich $CN_x$ showed desirable photocatalytic performance in the degradation of organics from high-salt wastewater. In high-salt wastewater, the salt often occupied the surface sites of catalyst, to stop the adsorption-oxidization of organics, resulting in the catalyst deactivation. To reactivate catalyst, it is washed several times with deionized water. In this study, the Zn-rich $CN_x$ showed a low adsorption capacity of 2,4-DCP, revealing that it had a few surface adsorption sites. Thereby, it also kept good photocatalytic performance in high-salt wastewater.

The Zn-rich $CN_x$ had a broad absorbance spectrum, and exhibited ability to adsorb more photon with different energy in such range. In addition, it had a ZnO-$CN_x$ heterojunction, to extend the migration distance of the light-induced electron-hole pair. This promoted the separation of light-induced electron-hole pair, resulting in the generation of adequate free radicals for oxidation/decomposition of organics. Thereby, the Zn-rich CNx showed high photocatalytic degradation rate of 2,4-DCP, in comparison with the other synthesized catalysts, e.g., Pb@BC-20%$TiO_2$, Cu/ZnS, ZnO, CuPc/g-$C_3N_4$ and Au/$TiO_2$/$PO_4$ (Table 1). In the photocatalytic degradation, the free radicals unselectively attacked 2,4-DCP and other organics, including rhodamine B, atrazine and aniline pollutants . Thus, the Zn-rich $CN_x$ posed bright application prospect in the wastewater treatment in paper, printing and dyeing, pharmaceutical and pickled food industries [11,12].

**Table 1.** 2,4-DCP degradation by Zn-rich $CN_x$ in comparison with the other materials.

| No. | Light | Catalyst | Experimental condition | Rate mg/L/min | Ref. |
|---|---|---|---|---|---|
| 1 | 300W HP | 0.1 g/L Pb@BC-20%$TiO_2$ | $C_0$=100 mg/L，240 min | 0.40 | [13] |
| 3 | 300W HID | 0.4 g/L Cu/ZnS | $C_0$=16 mg/L，pH=4，150min | 0.07 | [14] |
| 4 | 1 mW/cm² UV | 0.1 g/L ZnO | $C_0$=80 mg/L，360min | 0.19 | [15] |
| 5 | 300W HID | 2.5 g/L $CeO_2$/$TiO_2$/MOF | $C_0$=20 mg/L，150min | 0.12 | [16] |
| 6 | 150 W HW | 0.4 g/L R-rGO/$TiO_2$ | $C_0$=16.3 mg/L，60min，pH=6~7 | 0.26 | [17] |
| 7 | HID | 2.5 g/L CuPc/g-$C_3N_4$ | $C_0$=100 mg/L，240min | 0.33 | [18] |
| 8 | HID | 0.25 g/L Au/$TiO_2$/$PO_4$ | $C_0$=100 mg/L，240min | 0.42 | [19] |
| 9 | HID | 2.5 g/L Zn/BiFeO | $C_0$=10 mg/L，60min | 0.10 | [20] |

 doi:10.20944/preprints202405.1750.v1



| | | | | | |
|---|---|---|---|---|---|
| 10 | 400w MH，220 μW/cm² | 0.8 g/L S-$TiO_2$ | $C_0$=25 mg/L，240 min | 0.09 | [21] |
| 12 | 300W HID | 1 g/L $Ag_3PO_4$/$BiVO_4$ | $C_0$=20 mg/L，180 min | 0.09 | [22] |
| 13 | HP 365nm | 0.1 g/L Zn-$CN_x$ | $C_0$=100 mg/L，120 min | 0.63 | This work |

HP:mercury lamp; HID: xenon lamp; UV: ultraviolet light; HW: Incandescent lamp; MH: metal halide lamps.

Even though the Zn-rich $CN_x$ had many advantages in high-salt wastewater treatment, some investigation also should be taken in future. First, the stability of Zn-rich $CN_x$ should be optimized, including the leaching of Zn and the reusability in wastewater treatment. Second, the synthesis of Zn-rich CNx was tedious and energy-consuming. New synthesis method should be developed at mild condition to simplify the synthesis process and save energy. Third, costly reagents were used in the synthesis. The liquid reagents should be recycled, whilst the metallic chemical can be extracted from spent waste.

## 4. Conclusion

In summation, the process of high salinity tolerance of Zn-rich CNx in the photocatalytic treatment of wastewater had been studied and further corroborated. The results of the study showed that the degradation and Kobs of 2,4-DCP removal increased slightly with increasing salt content. Quenching experiment shown tha $\cdot O_2^-$ and ·OH played a important role. Combined with product analysis, the 2,4-DCP dehalogenation and ring-opening pathway was proposed. Moreover, the Zn@CN photocatalysis system also exhibited stability under initial pH interferences, 2,4-DCP concentration change. Overall, this study introduced a promising avenue for high salt organic wastewater treament in photocatalysis systems.

**Acknowledgments:** The authors acknowledge funding from the National Natural Science Foundation of China (52370158 and 52070038), the Science and Technology Program of Jilin Province (20240304153SF) and the Featured Innovation Project of Guangdong Provincial Department of Education (2023KTSCX050).

## Reference

1. Liang, Y, Jiao, C, Pan, L, Zhao, T, Liang, J, Xiong, J, Wang, S, Zhu, H, Chen, G, Lu, L, Song, H, Yang, Q, Zhou, Q. Degradation of chlorine dioxide bleaching wastewater and response of bacterial community in the intimately coupled system of visible-light photocatalysis and biodegradation. Environmental Research **2021**, *195*, 110840.
2. Xu, R, Chi, T, Ren, H, Li, F, Tian, J, Chen, L. The occurrence, distribution and removal of adsorbable organic halogens (AOX) in a typical fine chemical industrial park. Environmental Pollution **2022**, *312*, 120043.
3. Xie, Y, Chen, L, Liu, R. AOX contamination status and genotoxicity of AOX-bearing pharmaceutical wastewater. Journal of Environmental Sciences **2017**, *52*, 170-7.
4. Hu, D, Song, L, Yan, R, Li, Z, Zhang, Z, Sun, J, Bian, J, Qu, Y, Jing, L. Valence-mixed iron phthalocyanines/(100)$Bi_2MoO_6$ nanosheet Z-scheme heterojunction catalysts for efficient visible-light degradation of 2-chlorophenol via preferential dechlorination. Chemical Engineering Journal **2022**, *440*, 135786.
5. Wu, S, Liu, H, Lin, Y, Yang, C, Lou, W, Sun, J, Du, C, Zhang, D, Nie, L, Yin, K, Zhong, Y. Insights into mechanisms of UV/ferrate oxidation for degradation of phenolic pollutants: Role of superoxide radicals. Chemosphere **2020**, *244*, 125490.
6. Erhardt, C S, Basegio, T M, Capela, I, Rodríguez, A L, Machado, Ê L, López, D A R, Tarelho, L, Bergmann, C P. AOX degradation of the pulp and paper industry bleaching wastewater using nZVI in two different agitation processes. Environmental Technology & Innovation **2021**, *22*, 101420.
7. Melliti, E, Touati, K, Abidi, H, Elfil, H. Iron fouling prevention and membrane cleaning during reverse osmosis process. International Journal of Environmental Science and Technology 2019, 16(7), 3809-18.
8. Garg, S, Xu, Q, Moss, A B, Mirolo, M, Deng, W, Chorkendorff, I, Drnec, J, Seger, B. How alkali cations affect salt precipitation and $CO_2$ electrolysis performance in membrane electrode assembly electrolyzers. Energy & Environmental Science 2023.
9. Ali, S, Humayun, M, Pi, W, Yuan, Y, Wang, M, Khan, A, Yue, P, Shu, L, Zheng, Z, Fu, Q, Luo, W. Fabrication of $BiFeO_3$-g-$C_3N_4$-$WO_3$ Z-scheme heterojunction as highly efficient visible-light photocatalyst for water reduction and 2,4-dichlorophenol degradation: Insight mechanism. J Hazard Mater **2020**, *397*, 122708.

 doi:10.20944/preprints202405.1750.v1




10. Haider, M R, Jiang, W, Han, J, Mahmood, A, Djellabi, R, Liu, H, Asif, M B, Wang, A. Boosting Hydroxyl Radical Yield via Synergistic Activation of Electrogenerated HOCl/$H_2O_2$ in Electro-Fenton-like Degradation of Contaminants under Chloride Conditions. Environmental Science & Technology 2023, 57(47), 18668-79.
11. Tang, R, Zeng, H, Gong, D, Deng, Y, Xiong, S, Li, L, Zhou, Z, Wang, J, Feng, C, Tang, L. Thin-walled vesicular Triazole-CN-PDI with electronic n→π* excitation and directional movement for enhanced atrazine photodegradation. Chemical Engineering Journal **2023**, *451*, 138445.
12. Liang, H, Bai, J, Xu, T, Li, C. Enhancing photocatalytic performance of heterostructure $MoS_2$/g-$C_3N_4$ embeded in PAN frameworks by electrospining process. Materials Science in Semiconductor Processing 2021.
13. Lu, X. Performance study of metal-rich biochar modified $TiO_2$ for photocatalysis and activation of sodium persulfate; Shenyang University of Aeronautics and Astronautics, 2020.
14. Sun, J, Ji, X, Jiang, G, Liu, F, Li, F. Photocatalytic degradation of 2,4-dichlorophenol by Cu-doped ZnS nanomaterials; proceedings of the Chinese Society of Environmental Science 2022 Annual Scientific and Technical Conference - Environmental Engineering Technology Innovation and Application Session, Nanchang, Jiangxi, China, F, 2022.
15. Limón-Rocha, I, Guzmán-González, C A, Anaya-Esparza, L M, Romero-Toledo, R, Rico, J L, González-Vargas, O A, PérezLarios, A. Effect of the Precursor on the Synthesis of ZnO and Its Photocatalytic Activity. Inorganics 2022, 10(2), 1-18.
16. Muhammad, H, Lang, S, Wenbo, P, Hui, X, Abbas, K, Zhiping, Z, Qiuyun, F, Yahui, T, Wei, L. Vertically grown $CeO_2$ and $TiO_2$ nanoparticles over the $MIL_{53}$Fe MOF as proper band alignments for efficient $H_2$ generation and 2,4-DCP degradation. Environmental science and pollution research international 2022, 29(23), 34861-73.
17. Ramanathan, S, Thamilselvan, A, Radhika, N, Padmanabhan, D, Durairaj, A, Obadiah, A, Lydia, I S, Vasanthkumar, S. Development of rutin-rGO/$TiO_2$ nanocomposite for electrochemical detection and photocatalytic removal of 2,4-DCP. Journal of the Iranian Chemical Society 2021, 18(9), 1-16.
18. Guo, Y, Li, J, Guo, C, Cong, S, Yang, X. Preparation and photocatalytic degradation of 2,4-dichlorophenol by CuPc/g-$C_3N_4$. Chemical Engineer 2020, 34(08), 4-6.
19. Ali, S, Li, Z, Ali, W, Zhang, Z, Wei, M, Qu, Y, Jing, L. Synthesis of Au-decorated three-phase-mixed $TiO_2$/phosphate modified active carbon nanocomposites as easily-recycled efficient photocatalysts for degrading high-concentration 2,4-DCP. RSC Advances 2019, 9(66), 38414-21.
20. Humayun, M, Zheng, Z, Fu, Q, Luo, W. Photodegradation of 2,4-dichlorophenol and rhodamine B over n-type ZnO/p-type $BiFeO_3$ heterojunctions: detailed reaction pathway and mechanism. Environmental science and pollution research international 2019, 26(17), 17696-706.
21. Alalm, M G, Samy, M, Ookawara, S, Ohno, T. Immobilization of S-$TiO_2$ on reusable aluminum plates by polysiloxane for photocatalytic degradation of 2,4-dichlorophenol in water. Journal of Water Process Engineering **2018**, *26*, 329-35.
22. Qi, X, Gu, M, Zhu, X, Wu, J, Wu, Q, Long, H, He, K. Controlled synthesis of $Ag_3PO_4$/$BiVO_4$ composites with enhanced visible-light photocatalytic performance for the degradation of RhB and 2, 4-DCP. Materials Research Bulletin **2016**, *80*, 215-22.